THE OXIDATION RATES OF ARSENOPYRITE AND CHALCOPYRITE IN ACIDIC FERRIC CHLORIDE SOLUTIONS AT 0 TO 60°C

by

Patrick Michael Gagen

Thesis submitted to the Faculty of
Virginia Polytechnic Institute and State University
in partial fulfillment of the requirements of the degree of

MASTER OF SCIENCE

In

Geology

APPROVED:

J. D. Rimstidt, Chairman

J. R. Craig

R. J. Bodnar

May, 1987

Blacksburg, Virginia

THE OXIDATION RATES OF ARSENOPYRITE AND CHALCOPYRITE IN ACIDIC FERRIC CHLORIDE SOLUTIONS AT 0 TO 60°C

by

Patrick Michael Gagen

(ABSTRACT)

The rates of oxidation of arsenopyrite and chalcopyrite by Fe^{3+} at concentrations of 10^{-2} to 10^{-5} molal with a pH near 2 and temperatures of 0 to 60°C, conditions similar to those found in weathering sulfide ore deposits, have been determined. The rate equations for 25°C are:

$$dn_{Fe}3+/dt = 1.9\pm0.4 \times 10^{-7} (A) (m_{Fe}3+)^{0.43\pm0.01}$$

$$dn_{Fe}3+/dt = 1.5\pm0.6 \times 10^{-3} (A) (m_{Fe}3+)^{0.94\pm0.04}$$

for chalcopyrite and arsenopyrite respectively. The E_a of chalcopyrite is 63±2 kJ mol^{-1} (40 - 60°C). The E_a of arsenopyrite varied with temperature from 18±2 kJ mol^{-1} (0 - 25°C) to -6±2 kJ mol^{-1} (25 - 60°C).

Acknowledgments

I would like to acknowledge the many people who helped make this work possible. First, I thank my advisor and mentor Dr. J. D. Rimstidt for his invaluable help, guidance and encouragement through my studies, research and writing of this work. I would also like to thank my other committee members, Dr. J. R. Craig and Dr. R. J. Bodnar for their comments and review of this paper. Great appreciation goes to John Chermak and Billy Newcomb for their invaluable suggestions and help in the laboratory. I also thank Jim Light and Don Bodell for their technical and mechanical assistance with laboratory apparatus. Thanks also goes to all my past professors whose instruction has helped me attain this goal. I would also like to extent great appreciation to my family (Jim and Bonnie Gagen and brothers and sisters) and especially to my wife, Teresa, for their encouragement and assistance over the years.

The research was supported by NSF Grant Number EAR-8318998 and by the Department of the Interior's Mining and Mineral Resources Research Institute's program administered by the Bureau of Mines under allotment grant number G1164151.

Table of Contents

List of Tables

List of Figures

INTRODUCTION

The natural oxidation of sulfide minerals is a complex process. In most cases, it is initiated by the oxidation of pyrite by O_2 which releases Fe^{2+} and lowers the pH. *Thiobacillus ferrooxidans*, which flourish in acidic solutions, catalyze the oxidation of Fe^{2+} to Fe^{3+} which, in turn, reacts with more pyrite and other sulfide minerals to oxidize sulfide to sulfate. This process continues to release H^+ so the pH is maintained between one and three. The oxidation of sulfide minerals often leads to environmental degradation as a result of the release of H^+, Cu^{2+}, Pb^{2+}, SO_4^{2-} and AsO_4^{3-}; however, under controlled conditions, this process can be used for the economic recovery of metals from low grade ores. In addition, the metallic ions released to solution may be used in geochemical prospecting for ore deposits.

The purpose of this study was to determine the rates of oxidation of arsenopyrite and chalcopyrite by Fe^{3+} at a pH near 2 and temperatures of 0 to 60°C, conditions similar to those found in weathering sulfide ore deposits. These experiments were performed with concentrations of Fe^{3+} ranging from 10^{-2} to 10^{-5} molal which are typical of acid mine waters (Berner 1970).

A mixed flow reactor (MFR) was used to measure the rates of oxidation of chalcopyrite because it produces the most unambiguous results (Rimstidt and Dove 1986). Mixed flow reactor experiments determine the rate of reaction directly while data from plug flow and batch reactors must be fitted to assumed integrated rate functions. A detailed discussion and experimental design of the mixed flow reactor used can be found in Rimstidt and Dove (1986). A modified batch reactor experiment (the initial rate method used by McKibben and Barnes 1986) was used to measure the oxidation rates of arsenopyrite to avoid complexities resulting from the precipitation of scorodite ($FeAsO_4 \cdot 2H_2O$) on the arsenopyrite surfaces.

The most probable reactions involved in these oxidation experiments are:

$$FeAsS + 14Fe^{3+} + 10H_2O \Rightarrow 14Fe^{2+} + SO_4^{2-} + 16H^+ + FeAsO_4 \cdot 2H_2O \quad (1)$$

and

$$CuFeS_2 + 4Fe^{3+} \Rightarrow Cu^{2+} + 5Fe^{2+} + 2S^\circ \quad (2)$$

or

$$CuFeS_2 + 16Fe^{3+} + 8H_2O \Rightarrow Cu^{2+} + 17Fe^{2+} + 2SO_4^{2-} + 16H^+ \quad (3)$$

There have been several studies of the oxidation rates of chalcopyrite under various conditions (Table 1); however, most were designed to improve the hydrometallurgical recovery of copper and thus few were performed for conditions that simulate those found in nature. Most of these studies indicated reaction (2) as the dominant reaction under these more intense oxidizing conditions; however, no sulfur production was observed in the present experiments indicating that reaction (3) is the most probable reaction under the less oxidizing conditions found during weathering. Arsenopyrite oxidation has been studied to a lesser degree and there are no reported values of rate constants or activation energy, (Table 2). This study allows a comparison of the oxidation rates of various sulfide minerals (Chermak 1986, Walsh and Rimstidt 1986, and Wiersma and Rimstidt 1984) along with the effect of changing composition of the sulfide minerals in the series $CuFeS_2$-FeS_2-FeAsS, since pyrite has already been studied under these conditions (Wiersma and Rimstidt, 1984 and Newcomb, personal communication).

TABLE 1. PREVIOUS CHALCOPYRITE OXIDATION STUDIES

REACTANTS	PRODUCTS	NOTES	T & E_a*	REFERENCE
$CuFeS_2$, $FeCl_3$	CuCl, $FeCl_2$, S	Dependent on particle size, T, and $FeCl_3$/ $CuFeS_2$.	30°, 55°, 80°, 106°C	Haver and Wong (1971)
$CuFeS_2$, OH^-, O_2	Cu^{2+}, Fe^{3+}, S, H_2O	Dependent on T & pH. pH=0.25-2.	50-150°C	Leach and Braun (1975)
$CuFeS_2$, H_2SO_4, O_2, H_2O	$CuSO_4$, S, $Fe(OH)_3$	Linear kinetics, rate constant given as function of P_{O2} and T. (oxygen P in psi) $K_l=(2.82*10^{11}*10^{-7750/T}* P_o)$ $/(1+2.16*10^{10}* 10^{-5560/T}*P_o)$	125°-175°C	Yu, *et al.* (1973)
$CuFeS_2$, Fe^{3+}	Cu^{2+}, Fe^{2+}, S	First order; depdt. on $FeCl_3$ conc., T, and particle size rate=K_sA	75-96°C 41 kJ mol^{-1}	Palmer, *et al.* (1981)
$CuFeS_2$, NH_3, O_2, OH-	$Cu(NH_3)_4^{2+}$ Fe_2O_3, H_2O SO_4^{2-}	Depends on stirring rate for rates < 3000 rpm. pH=10.2	90°C, Ea= 41.84 kJ mol^{-1}	Beckstead and Miller (1977)
$CuFeS_2$, Fe^{3+}	Cu^{2+}, Fe^{2+}, S	Shrinking core kinetics. Catalyzed X4 by carbon	90°C, 68-84 kJ mol^{-1}; 113 kJ mol^{-1} with carbon.	Wan, *et al.* (1984)
$CuFeS_2$, Fe^{3+}	Cu^{2+}, S, Fe^{2+}	Catalyzed X3 by carbon.	90°C, E_a= 38.1 mol with carbon	Wan, *et al.* (1985)
$CuFeS_2$, Fe^{3+}	Cu^+, Fe^{2+}, S	Catalyzed by Cl^-; Shrinking core kinetics.		Habashi (1978)

TABLE 1. (CONTINUED) PREVIOUS CHALCOPYRITE OXIDATION STUDIES

REACTANTS	PRODUCTS	NOTES	T & E_a*	REFERENCE
$CuFeS_2$, Fe^{3+}	Cu^{2+}, S, Fe^{2+}	Catalyzed X3 by carbon. above. Rate dept. on transp. of e^- through the S layer.	60°, 75°, and 90°C 83.7 and E_a(shrink core) =96.3 kJ mol^{-1}	Munoz, *et al.* (1979)
$CuFeS_2$, + $Fe_2(SO_4)_3$ or $FeCl_3$	$CuSO_4$ or $CuCl + FeCl_3$ or $FeSO_4$ + S°	Sulfate inhibits rxn. Bornite impurities raise E_a	45-100°C 42 kJ mol^{-1} in Cl, 75 kJ mol^{-1} in SO_4^{2-}.	Dutrizac, (1981)
$CuFeS_2$, HCl, O_2	$CuCl_2$, S, FeOOH, H_2O	Cl^- catalyzes the reaction.	90-130°C 36 kJ mol^{-1}	Habashi and Tej Toor (1979)

*T = reaction temperature, °C; E_a = activation energy, kJ mol^{-1}.

TABLE 2. PREVIOUS ARSENOPYRITE OXIDATION STUDIES

REACTANTS	PRODUCTS	NOTES	TEMP.	REFERENCE
FeAsS, Fe^{3+}, H_2O	Fe^{2+}, SO_4^{2-}, $FeAsO_4 \cdot H_2O$, H^+	Catalyzed by ferrooxidans bacteria. This reaction is hypothesized for formation of scorodite.		Dove & Rimstidt (1985)
FeAsS, O_2, H_2O	$FeAsO_4$, H_2SO_4	Catalyzed by *Thiobacillus ferrooxidans*. Surface area is an important factor	25-40°C	Pinches (1975)

EXPERIMENTAL PROCEDURE

Arsenopyrite and chalcopyrite used in these experiments were obtained from Ward's Natural Science Establishment, Inc. The chalcopyrite came from Messina, Transvaal, Republic of South Africa and the arsenopyrite came from Gold Hill, Utah. The mineral samples were prepared by first breaking the bulk material into one to two centimeter size pieces and hand sorting to remove macroscopic impurities (mostly silicates). The high grade material was crushed and sieved and the 60-100 mesh size fraction was retained for the experiments. The sieved sample was rinsed five times in ethanol, to remove the very fine particles which adhere to the grains, and then air dried. The arsenopyrite was processed as stated above except that an 18 inch "Gold Hound Goldwheel" was employed to remove the silicate gangue which made up approximately 25% of the sample. This apparatus separated the grains on the basis of density. Microscopic examination of the processed sample revealed no contaminating silicates. The mineral grains were examined in polished section and the chalcopyrite was found to contain minor (<1%) sulfide contaminants (pyrite and covellite) and the arsenopyrite was free of contaminants. The minerals were analyzed by electron microprobe (Table 3) and the formulae were found to be $CuFeS_2$ for chalcopyrite and $FeAs_{0.95}S_{1.05}$ for arsenopyrite. The surface area, determined by N_2 adsorption, was 0.049 $m^2\ g^{-1}$ for the unreacted chalcopyrite and 0.066±0.02 $m^2\ g^{-1}$ for the unreacted arsenopyrite (Appendix I).

Ferric chloride solutions were prepared by mixing appropriate aliquots of a 0.5 molal ferric chloride stock solution and concentrated HCl into distilled deionized water to obtain a final pH near 2. The ferric chloride stock solution was made by mixing 135.16 g of $FeCl_3 \cdot 6H_2O$ (Fisher Scientific lot #853551) and 250 ml of concentrated HCl and diluting to 1 liter with distilled deionized water. Ferric iron concentrations of the run solutions ranged from 10^{-2} to 10^{-5} molal. The pH was checked prior to each experiment. Ionic strengths of these solutions were sufficiently low to use the extended Debye-Huckel equation to estimate the

TABLE 3. COMPOSITIONS OF MINERALS USED IN THESE EXPERIMENTS AS DETERMINED BY ELECTRON MICROPROBE

Element	Arsenopyrite	Chalcopyrite
Iron	34.58 wt%	34.10 wt%
Copper	*	30.15
Arsenic	44.47	*
Sulfur	20.95	35.75

* not determined

activity coefficients and the speciation calculations were performed using a revised version of the program written by Wiersma (1982).

The mixed flow reactor (MFR) (Fig. 1) developed by Rimstidt and Dove (1986) was used for all chalcopyrite experiments and for some preliminary arsenopyrite experiments. For each experiment approximately two grams of the mineral sample were held between two 120 mesh nylon screens fixed in the center of a 2 inch (5 cm.) ID PVC pipe and coupling. This setup was then placed in a reaction kettle (free volume = 915 ml). The kettle was filled with ferric chloride solution, closed, and then placed into a water bath thermostated at the desired temperature. Ferric chloride solution was supplied to the reactor by a peristaltic pump at constant rates ranging from 5×10^{-5} to 7×10^{-6} kg sec^{-1}. The Eh of the effluent was measured using an Eh electrode in a flow cell down stream from the reactor kettle. The experiment was continued until the Eh reached a steady state. A 25 ml sample of the effluent solution produced under steady state conditions was sampled and saved for ICP analysis. The reactor kettle was opened and the mineral sample was removed, rinsed in distilled deionized water to arrest the reaction, dried, and stored in a desiccator.

Eh measurements were made using a Fisher Scientific combination platinum/4 molal KCl/Ag - AgCl Eh electrode and an Orion Research 811 meter. The electrode was calibrated against a standard Zobell solution as described by Langmuir (1971), using the temperature correction equation from Nordstrom (1977). The calibration adjustment for these experiments was:

$$Eh = \text{emf (volts)} + 0.19635 \text{ (volts)} \quad (4)$$

The ferric ion content of the effluent was calculated from the following equations:

$$Eh = E^\circ + (RT/nF) \ln(a_{Fe}3+/a_{Fe}2+) \quad (5)$$

$$T_{Fe} = m_{Fe}3+ + m_{Fe}2+ \quad (6)$$

$$a_{Fe}3+ = \gamma_{Fe}3+ m_{Fe}3+ \quad (7)$$

$$a_{Fe}2+ = \gamma_{Fe}2+ m_{Fe}2+ \quad (8)$$

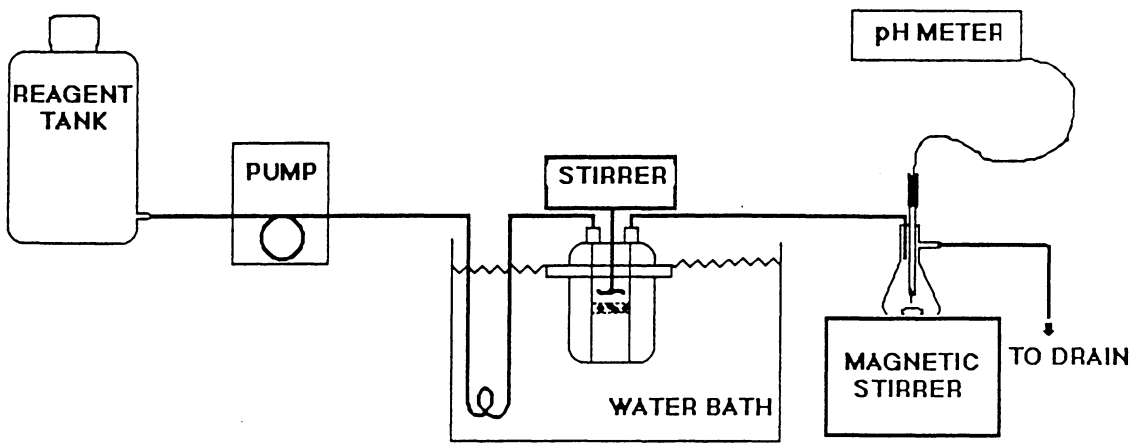

FIG. 1. Schematic diagram of the mixed flow reactor (MFR) system.

where T_{Fe} is the total iron concentration of the solution. Then combining equations (5) through (8) gives

$$m_{Fe^{3+}} = (T_{Fe}(\gamma_{Fe^{2+}}/\gamma_{Fe^{3+}})\, e^{(Eh-E^\circ)nF/RT}) / (1+(\gamma_{Fe^{2+}}/\gamma_{Fe^{3+}})e^{(Eh-E^\circ)nF/RT}) \quad (9)$$

The derivation of this equation is given in Wiersma and Rimstidt (1984). The apparent rate of reduction of Fe^{3+}, r', was found by multiplying the difference between the Fe^{3+} concentration in the feed solution and the effluent solution, dn/M (mol kg^{-1}) by the flow rate M/dt (kg sec^{-1}) (Levenspiel 1972).

$$r' = (dn/dt)_{rxn} = [(n/M)_{in} - (n/M)_{out}][M/dt] = (dn/M)(M/dt) \quad (10)$$

The actual rate was then calculated from the apparent rate as follows:

$$r = r'/(\text{sample mass, g})(\text{specific surface area, } m^2\, g^{-1}) \quad (11)$$

This experiment worked well for chalcopyrite; however, the results for arsenopyrite were unusual, in that, the rates measured at 60°C were slower than the rates at 40°C (Appendix II). Light microscope and SEM examination (Fig. 2) of the reacted grains showed significant although not continuous scorodite deposits on the grain surfaces. In order to determine whether, over the rather long duration of the mixed flow reactor experiments (from nine to 23 hours), a scorodite layer might form and inhibit the reaction, a series of batch reactor experiments of short duration (40 minutes) were performed. A schematic diagram of the batch reactor used is shown in Figure 3. The arsenopyrite was held in a PVC sample holder similar to the one used in the MFR system. This mount was shorter (11.4 cm. instead of 16.5 cm.) so the entire sample holder was completely submerged in the 500 ml of solution used in these experiments. A stirrer with the same type blade used in the MFR circulated the solution downward through the mesh that held the arsenopyrite grains. The Eh electrode was mounted in the kettle outside of the sample holder. This entire apparatus and the ferric chloride solution were thermally equilibrated in the water bath before the 500 ml of ferric chloride solution was poured into the reactor kettle to initiate the reaction. The emf readings, recorded at 5 minute intervals, were converted to $m_{Fe^{3+}}$ using equations (4) and (9).

FIG. 2. Scanning Electron Photomicrographs of arsenopyrite grains reacted in the mixed flow reactor at 40°C for 23 hours in 10^{-2} Fe^{3+} solution. (a) The scale bar is 100 μm long. The boytriodial deposits on the grain in the lower left are scorodite. (b) The scale bar is 10 μm long. This is a closer view of the scorodite deposits.

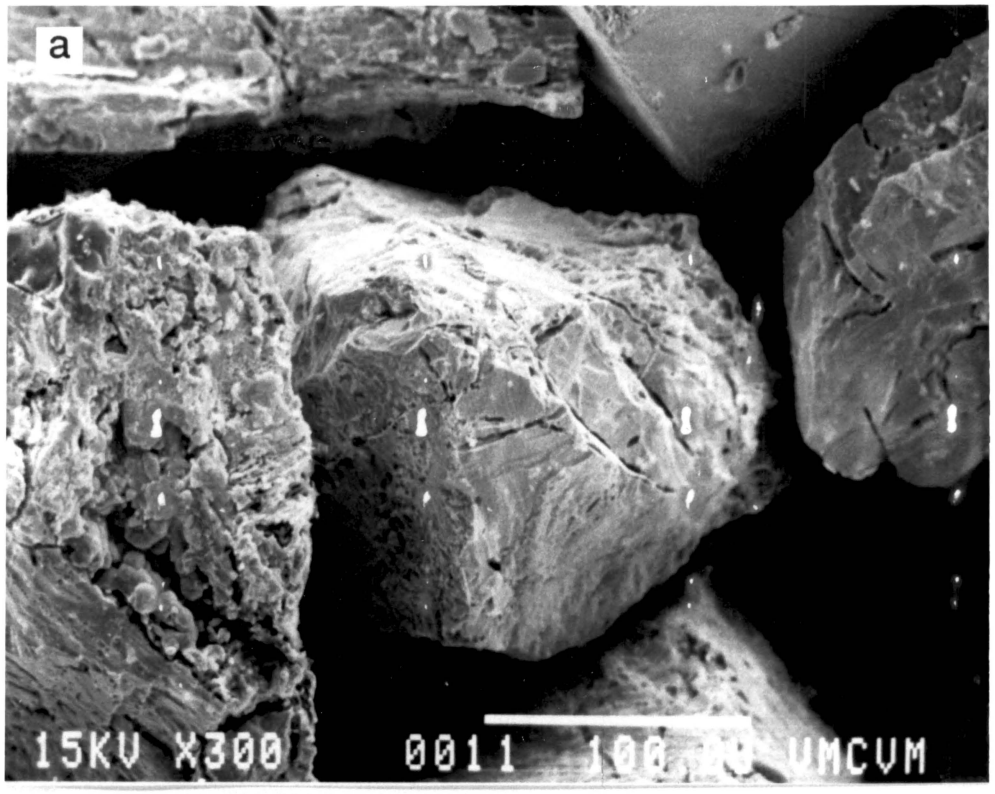
a
15KV X300
0011
VMCVM

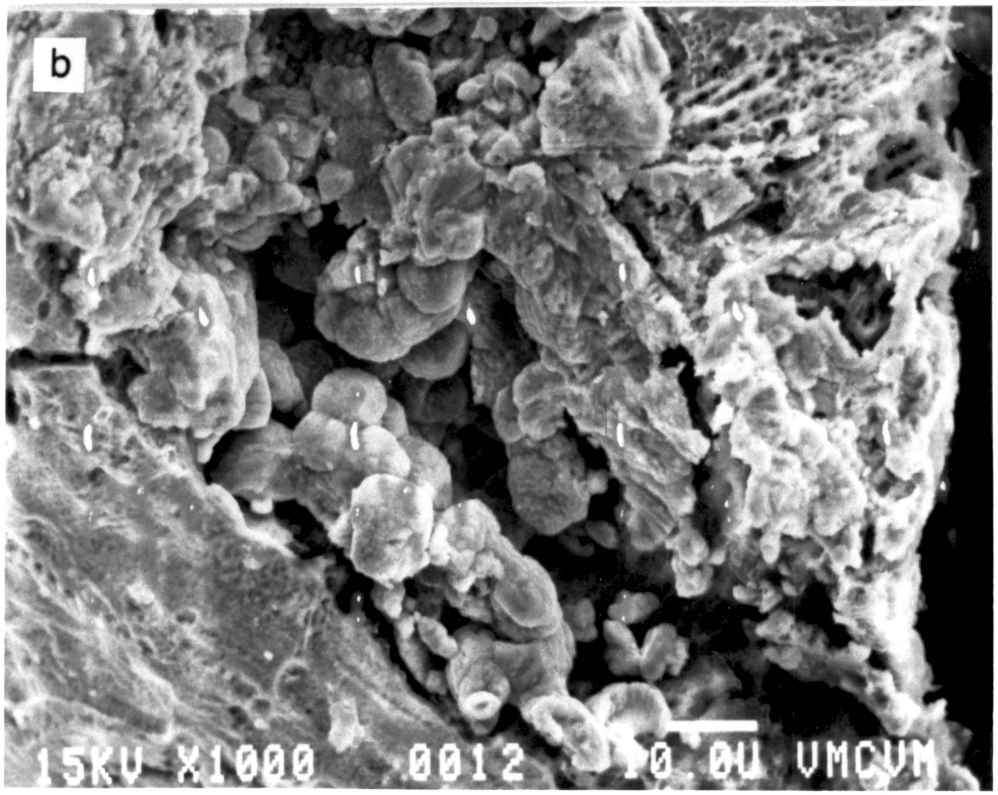
b
15KV X1000
0012
VMCVM

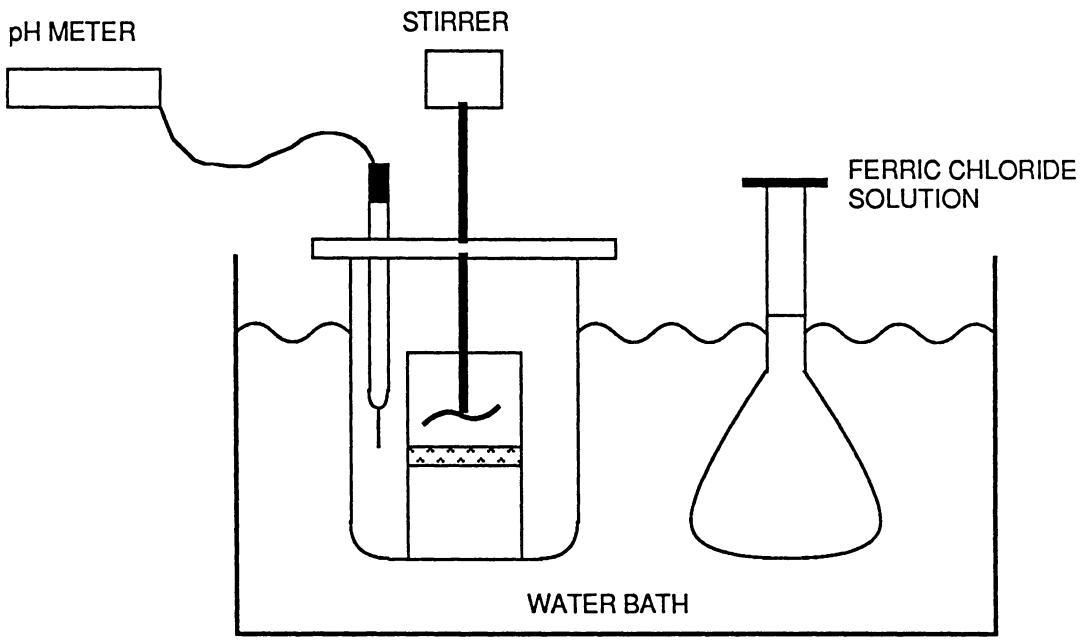

FIG. 3. Schematic diagram of the batch reactor system.

The initial rate method described by McKibben and Barnes (1986) was used to calculate the apparent rate constant, r', which was then converted to the rate constant, r, using equation (11).

In order to determine whether the results obtained using the initial rate method, the integrated rate model, and the mixed flow reactor are consistent, a variety of measurements of the rate of oxidation of pyrite by ferric iron were compared (Table 4). This shows that the initial rate method used in this study yields results consistent with other rate studies.

The specific surface area of samples of the reacted mineral grains was determined from a two or three point N_2 BET isotherm obtained using a Quantasorb surface area analyzer. In all cases, a sample of approximately 0.2 g was outgassed at 50°C for four to six days. Two of the most reacted and two of the least reacted chalcopyrite samples were selected along with four others chosen at random. For the chalcopyrite samples the error for the individual measurements was found to be greater than the variance of all of the surface area measurements; therefore all values were averaged to give an average specific surface area of 0.030±0.013, (see Appendix III). Specific surface areas of the arsenopyrite samples from the mixed flow reactor experiments were also determined, (see Appendix IV). Note that the surface area of the unreacted sample is required to normalize the rate constants determined by the initial rate method.

TABLE 4. RATES OF OXIDATION OF PYRITE BY 10^{-3} m Fe^{3+} AT 25°C AND pH = 2.

Log r mol m^{-2} sec^{-1}	Method	Source
-6.91	initial rate	McKibbin and Barnes (1986)
-6.53	initial rate	this study
-6.57	integrated*	Wiersma and Rimstidt (1984)
-6.73	integrated*	this study
-6.67	mixed flow reactor	Newcomb (pers. comm.)

* Fit to first order rate law.

RESULTS

The chalcopyrite reaction rates measured in this study are given in Table 5 and plotted as log rate versus log $m_{Fe}3+$ (Fig. 4), the parameters for these plots are in Table 6. The arsenopyrite reaction rates measured in this study are given in Table 7 and plotted in Figure 5 with the parameters in Table 8. These results show that the chalcopyrite oxidation rates are over two orders of magnitude lower than those of arsenopyrite. The slope of the lines on these plots gives the reaction order in terms of $m_{Fe}3+$. The reaction order for chalcopyrite is 0.43±0.01 and for arsenopyrite is 0.94±0.04. Figure 6 is an Arrhenius plot for chalcopyrite and Figure 7 is an Arrhenius plot for arsenopyrite. The activation energy of chalcopyrite, calculated from Figure 6, is 63±3 kJ mol^{-1}. Figure 7 shows that the Arrhenius plot for arsenopyrite does not produce the expected straight line with a positive slope. From 0 to 25°C the E_a is ≈ 18±2 kJ mol^{-1} and from 25 to 60°C the E_a is ≈ -6±2 kJ mol^{-1}. The significance of this behavior will be discussed later. The rate equations for 25°C as calculated from the data in Tables 5 & 6 are

$$dn_{Fe}3+/dt = 1.9\pm0.4 \times 10^{-7} (A) (m_{Fe}3+)^{0.43\pm0.01} \quad (12)$$

for chalcopyrite and

$$dn_{Fe}3+/dt = 1.5\pm0.6 \times 10^{-3} (A) (m_{Fe}3+)^{0.94\pm0.04} \quad (13)$$

for arsenopyrite.

SEM examination of reacted solids showed no detectable change of the surfaces of the chalcopyrite grains (Fig. 8) and minor scorodite formation on portions of the arsenopyrite grain surfaces from the MFR experiments (Fig. 9). Reflected light examination of the reacted grains showed no traces of covellite or other copper or iron sulfides on the chalcopyrite grains and no visible arsenic or iron sulfides on the arsenopyrite grains. Scorodite appears to by the only product of arsenopyrite oxidation by Fe^{3+} as predicted by reaction (1) and as observed in nature. Scorodite deposition was not extensive on the arsenopyrite grains

TABLE 5. CHALCOPYRITE REACTION RATES

RUN NUMBER	Fe^{3+} in molal	EMF volts	Fe^{3+} out molal	r_{flow} kg sec^{-1}	MASS * g	log r mol m^{-2} sec^{-1}
			60°C			
Cpy 16	1E-04	0.5732	5E-05	4.24E-05	1.9999	-7.454
Cpy 17	1E-04	0.5671	4.4E-05	4.78E-05	2.0000	-7.354
Cpy 20	1E-05	0.5129	8.6E-07	4.67E-05	2.0008	-8.153
Cpy 21	1E-05	0.5198	1.1E-06	4.90E-05	1.9996	-8.143
Cpy 22	3.2E-05	0.5525	9.7E-06	4.73E-05	2.0005	-7.767
Cpy 23	3.2E-05	0.5489	8.8E-06	4.88E-05	2.0004	-7.736
Cpy 29	3.2E-04	0.5990	2.3E-04	4.80E-05	2.0009	-7.170
			40°C			
Cpy 30	1E-04	0.5607	3.8E-05	7.86E-06	2.0016	-8.094
Cpy 31	3.2E-05	0.5379	6.3E-06	8.06E-06	2.0005	-8.474
Cpy 32	3.2E-05	0.5341	5.6E-06	8.06E-06	1.9997	-8.461
Cpy 33	1E-05	0.4985	5.1E-07	8.02E-06	1.9998	-8.901
Cpy 34	1E-05	0.4976	5E-07	8.15E-06	1.9995	-8.894
Cpy 35	1E-4	0.5559	3.4E-05	7.29E-06	2.0000	-8.098

*Mass of solid material used in each experiment. The specific surface area of the run products was 0.030 m^2 g^{-1} (Appendix III).

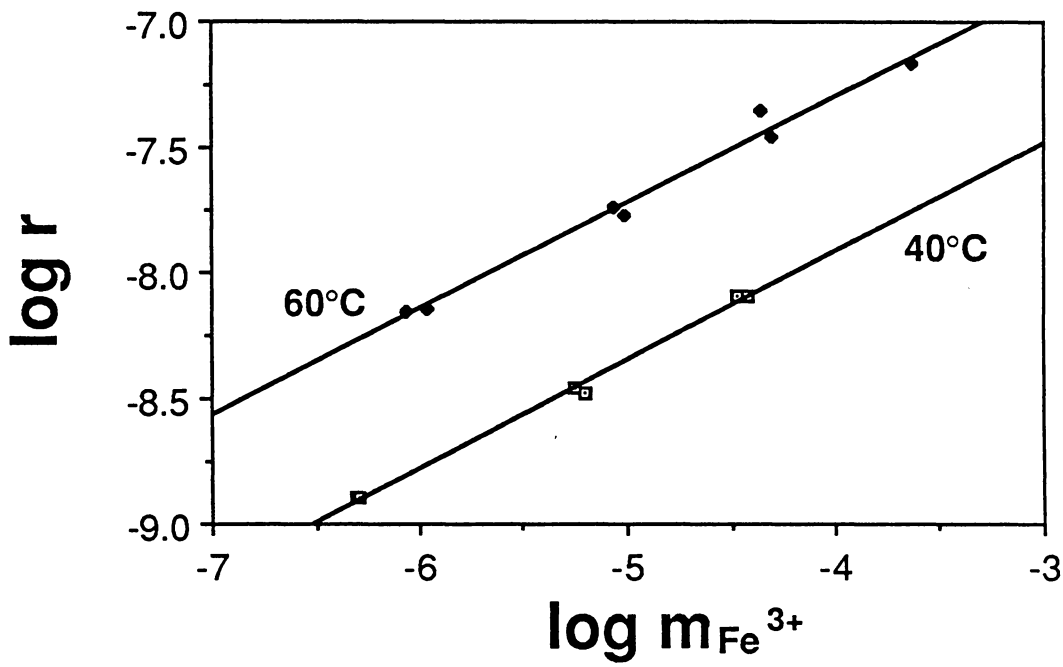

FIG. 4. Chalcopyrite oxidation rates plotted as log rate versus log $m_{Fe}3+$. The parameters of the equations of the best fit lines are given in Table 6.

TABLE 6. PARAMETERS FOR CHALCOPYRITE OXIDATION AT VARIOUS TEMPERATURES. [$r = k' (m_{Fe^{3+}})^n$]

TEMP.	n	log k	NUMBER OF POINTS	CORRELATION OF FIT
40°C	0.43±0.01	-6.19±0.07	6	1.00
60°C	0.42±0.02	-5.60±0.12	7	0.99

TABLE 7. ARSENOPYRITE REACTION RATES

RUN NUMBER	EMF volts	MASS[a] g	log Fe[b] molal	log r mol m^{-2} sec^{-1}
		0°C		
Aspy 71	0.5561	2.0004	-3.000	-6.189
Aspy 72	0.5359	2.0004	-3.498	-6.441
Aspy 73	0.5443	2.0002	-3.002	-6.145
Aspy 74	0.5435	2.0002	-3.506	-6.647
Aspy 75	0.5307	2.0003	-4.031	-6.991
Aspy 76	0.5382	2.0001	-4.043	-7.080
		15°C		
Aspy 68	0.5537	2.0004	-3.072	-6.056
Aspy 69	0.5499	2.0002	-3.564	-6.468
Aspy 70	0.5448	2.0005	-4.067	-6.929
		25°C		
Aspy 55	0.5601	2.0006	-3.100	-5.878
Aspy 56	0.5674	2.0001	-3.569	-6.399
Aspy 57	0.5491	2.0006	-4.132	-6.834
Aspy 58	0.5565	2.0002	-3.098	-5.855
Aspy 59	0.5496	2.0006	-3.657	-6.406
Aspy 61	0.5555	2.0005	-4.180	-6.976
		35°C		
Aspy 62	0.5758	2.0002	-3.171	-5.969
Aspy 63	0.5718	2.0005	-3.706	-6.474
Aspy 64	0.5682	2.0007	-4.291	-7.089
Aspy 65	0.5627	2.0001	-3.741	-6.450
Aspy 66	0.5646	2.0008	-4.278	-7.001
Aspy 67	0.5775	2.0000	-3.174	-6.965
		40°C		
Aspy 77	0.5953	2.0005	-3.125	-6.004
Aspy 78	0.5959	2.0010	-3.640	-6.575
Aspy 79	0.5820	2.0003	-4.265	-7.141
		60°C		
Aspy 81	0.6151	2.0007	-3.782	-6.666
Aspy 82	0.6139	2.0003	-4.231	-7.059
Aspy 83	0.5994	2.0008	-3.398	-6.259

a. Mass of solid used in each experiment. The specific surface area of the unreacted arsenopyrite was 0.066 m^2 g^{-1} (Appendix I).
b. Starting iron concentrations.

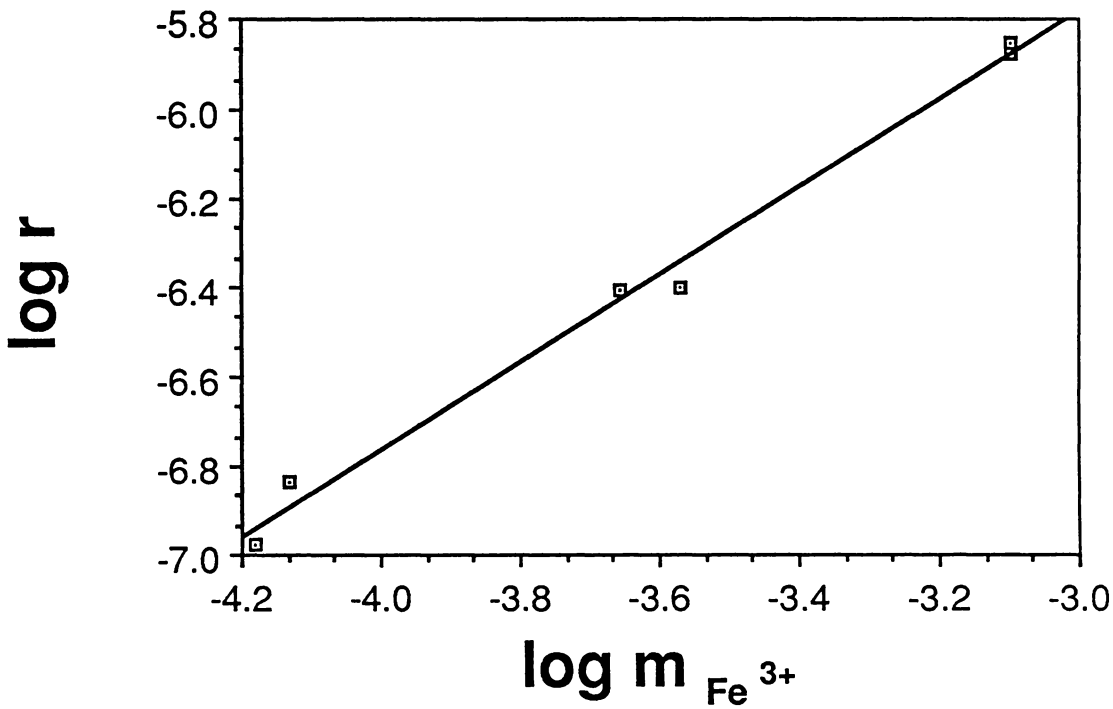

FIG. 5. The arsenopyrite oxidation rate at 25°C plotted as log rate versus log $m_{Fe}3+$. All of the lines are not plotted since they fall on top of each other due to the reversal in E_a's. The parameters of the equations of the best fit lines are given in Table 8.

TABLE 8. PARAMETERS FOR ARSENOPYRITE OXIDATION AT VARIOUS TEMPERATURES. [$r = k (m_{Fe}3+)^n$]

TEMP.	n	log k	NUMBER OF POINTS	CORRELATION OF FIT
0°C	0.84±0.08	-3.63±0.28	6	0.98
15°C	0.88±0.02	-3.35±0.08	3	1.00
25°C	0.98±0.04	-2.84±0.16	6	1.00
35°C	0.97±0.04	-2.88±0.14	6	1.00
40°C	0.99±0.06	-2.92±0.21	3	1.00
60°C	0.96±0.05	-3.02±0.20	3	1.00

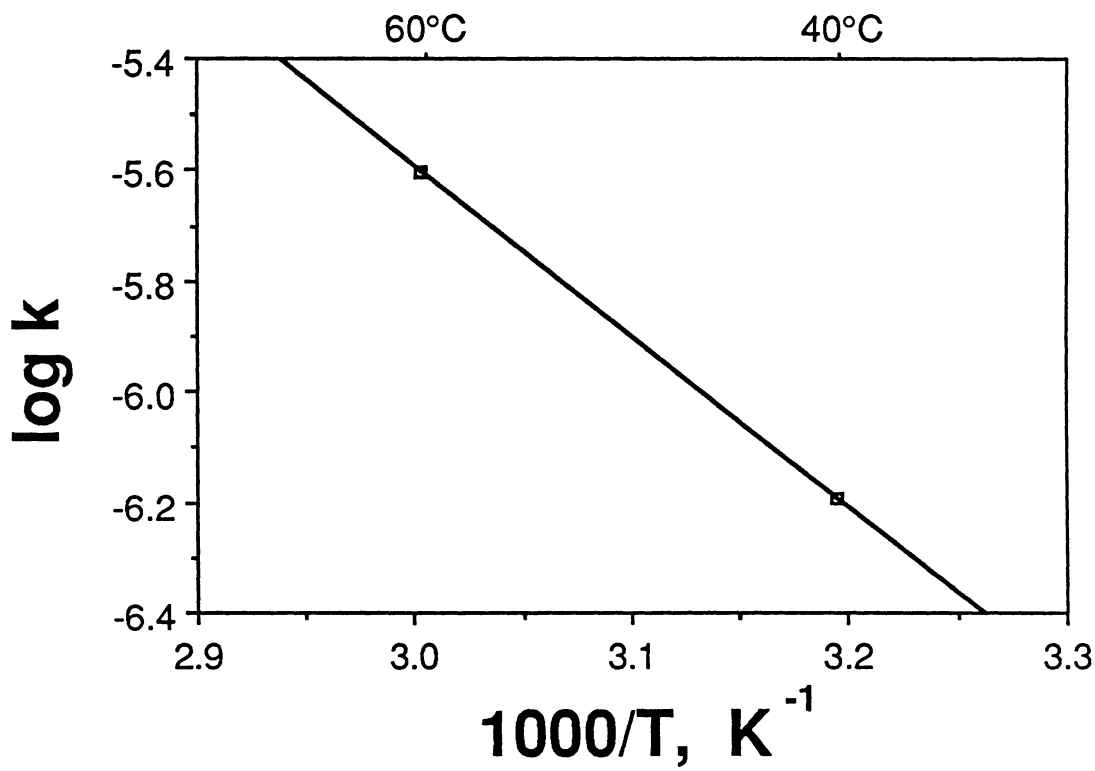

FIG. 6. Arrhenius plot for chalcopyrite. E_a = 63±3 kJ mol^{-1}.

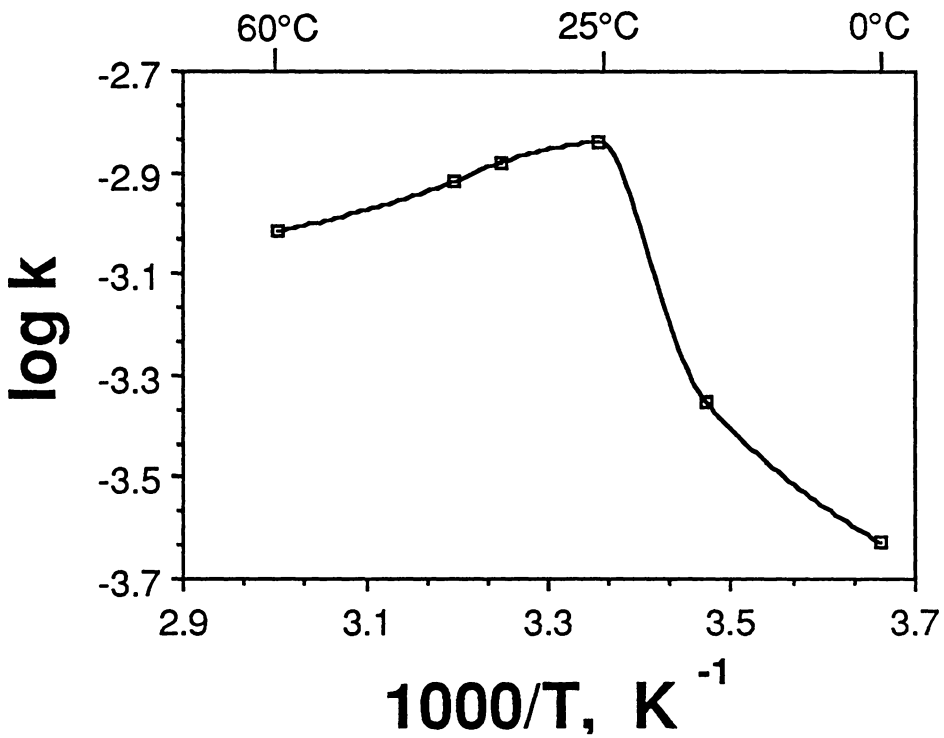

FIG. 7. Arrhenius plot for arsenopyrite. From 0-25°C the $E_a \cong 18$ kJ mol^{-1} and from 25-60°C the $E_a \cong -6$ kJ mol^{-1}.

FIG. 8. Scanning Electron Photomicrographs of (a) chalcopyrite starting material and (b) reacted chalcopyrite grains from run #16. Note that the extent of reaction of chalcopyrite was so low that these grains showed no significant change even after 14 hours of reaction at 40°C.

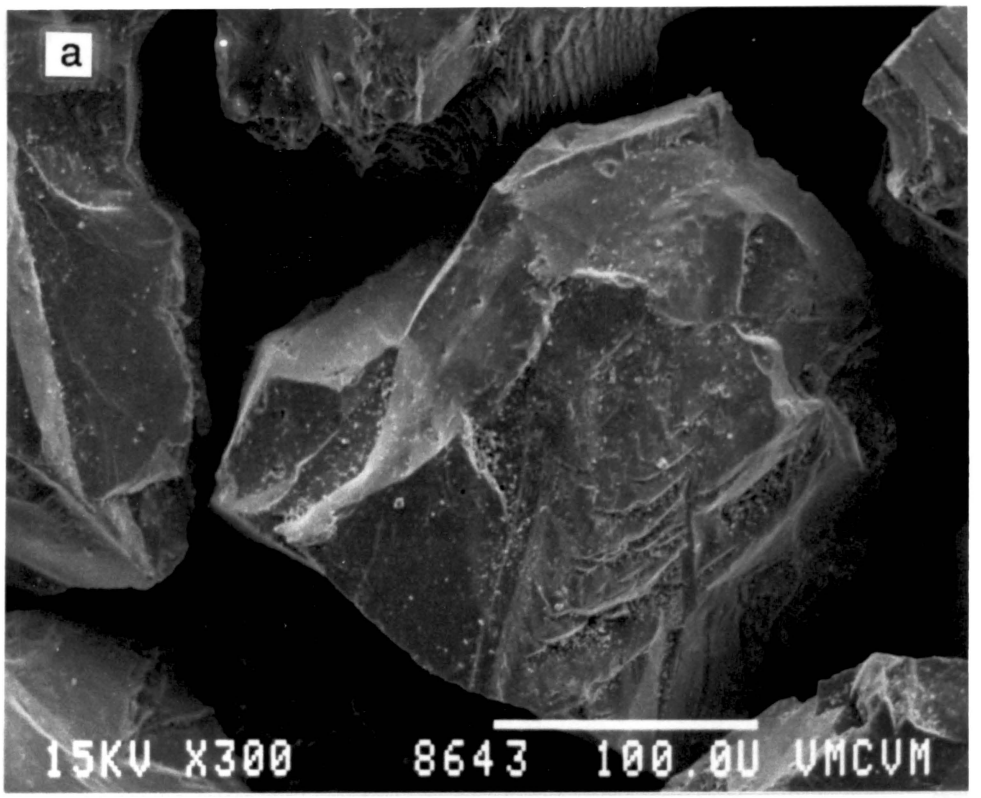
a
15KV X300 8643 100.0U VMCVM

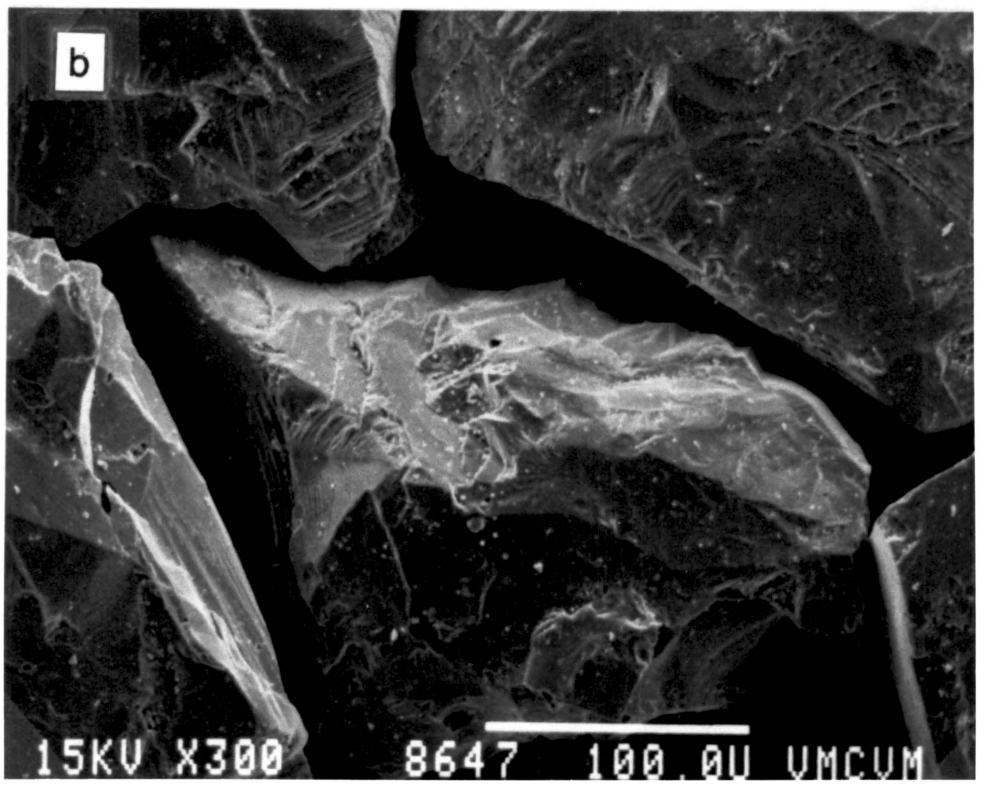
b
15KV X300 8647 100.0U VMCVM

FIG. 9. Scanning Electron Photomicrographs comparing (a) arsenopyrite starting material and (b) arsenopyrite grains reacted in the mixed flow reactor for nine hours at 60°C and a Fe^{3+} concentration of $10^{-3.5}$ m. Note the scorodite deposition and the development of etch pits. Fig. 2 shows details of scorodite deposition.

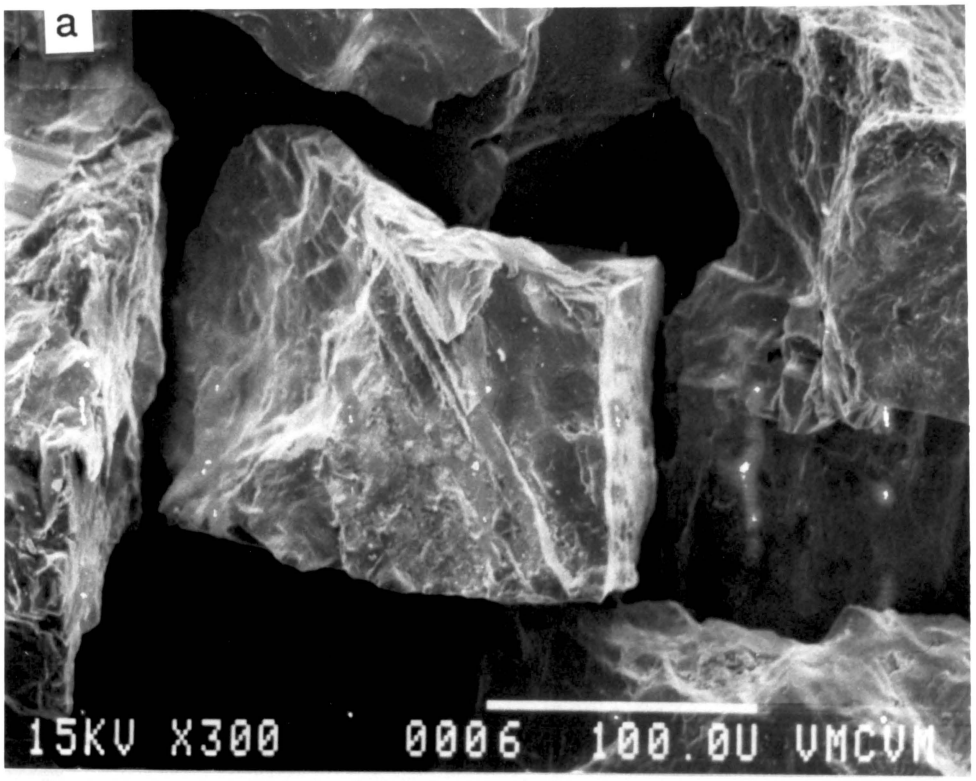
a
15KV X300 0006 100.0U VMCVM

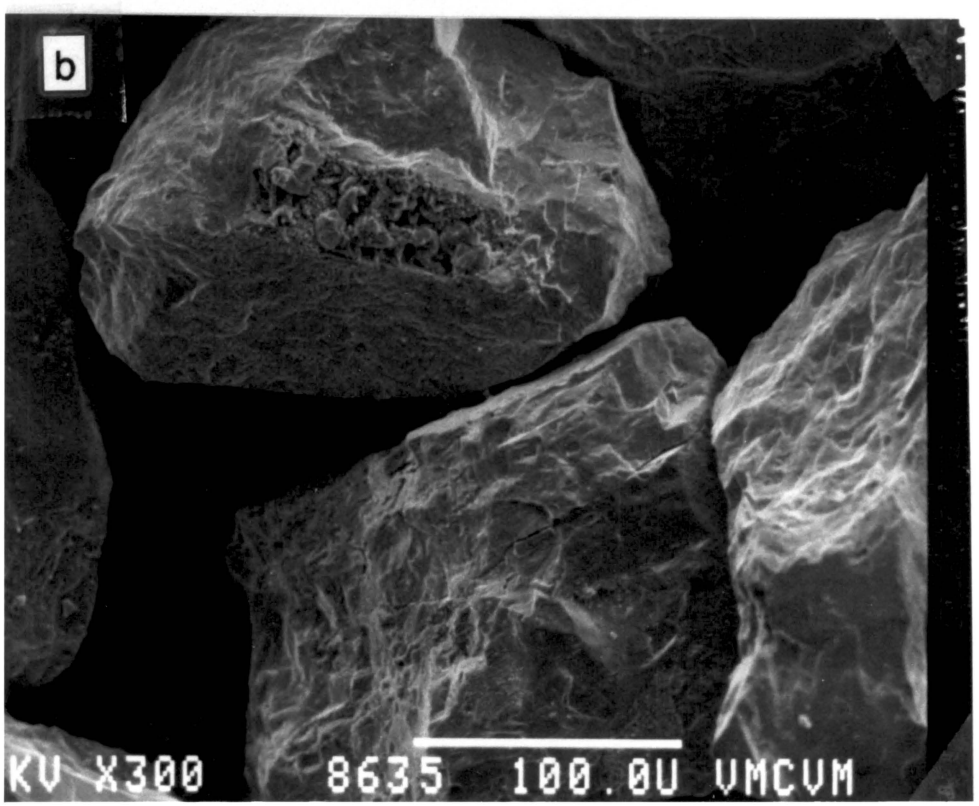
b
KV X300 8635 100.0U VMCVM

because of its relative high solubility in acidic solutions (Dove and Rimstidt 1985). The observed scorodite precipitated predominantly in cracks and sheltered areas where low flow velocities allowed the concentration of AsO_4^{3-} to build until scorodite saturation was exceeded. Elemental sulfur was not observed on either chalcopyrite or arsenopyrite suggesting that SO_4^{2-}, or at least some soluble sulfur anion was the dominant sulfur species produced and reactions 1 and 3 are the most probable reactions.

The concentrations of reaction products (sulfur, copper, iron, and arsenic) in the effluent from these experiments showed no simple, systematic relationship to the proposed reaction stoichiometries (Appendix V). It appears that either some elements were lost from solution by a non-systematic process or that although elemental sulfur was not precipitated some sulfur and arsenic species with an intermediate oxidation state were formed in the experiments. The lifetimes of such species in the acid, oxidizing solutions used here are unknown but are generally believed to be quite short.

CONCLUSIONS

Arsenopyrite, though commonly considered to be one of the most refractory of the ore minerals, has been found to undergo relatively rapid oxidation in acidic ferric chloride solutions. A comparison of oxidation rates may be seen in Table 9. The rates given in this table correspond to a ferric iron concentration of 10^{-3} molal and a temperature of 25°C. The table shows that arsenopyrite (FeAsS) oxidizes the fastest of the minerals studied and its oxidation rate is approximately one order of magnitude faster than for pyrite (FeS_2). On the other hand chalcopyrite ($CuFeS_2$) and covellite, oxidize more slowly than the minerals studied and chalcopyrite oxidizes 1.5 orders of magnitude slower than pyrite. This relationship suggests that perhaps, arsenic catalyzes the overall reaction while copper inhibits the oxidation reaction. For all the minerals studied to date, SO_4^{2-} is the dominant sulfur species produced at low ferric iron concentrations. This is consistent with observations in weathering sulfide deposits where elemental sulfur is rarely found. Note that the yellow sulfate minerals jarosite and copiapite, which are common in weathering sulfide deposits, are often misidentified as elemental sulfur.

The calculated E_a of chalcopyrite is 63±2 kJ mol^{-1} (40 - 60°C). This high E_a suggests a chemical reaction controlled mechanism rather than diffusion of Fe^{3+} through a product layer where the E_a would be less than ≈20 kJ mol^{-1} (Murray 1972). This is consistent with the reflected light and SEM observations which showed no product layer on the reacted chalcopyrite grains.

The activation energy of arsenopyrite varies dramatically over the temperature range considered. The E_a is ≈ 18 kJ mol^{-1} from 0 to 25°C and then becomes ≈ -6 kJ mol^{-1} from 25 to 60°C. The unusual negative E_a for arsenopyrite at temperatures above 25°C gives important information about the reaction mechanism. First, it is consistent with the suggestion that the reaction

TABLE 9. CHARACTERISTICS OF SULFIDE OXIDATION BY 0.001 m FERRIC IRON (pH=2) AT 25°C. LISTED IN ORDER OF MOST REACTIVE TO LEAST REACTIVE.

MINERAL	RATE mol m^{-2} sec^{-1}	ORDER	E_a kJ mol^{-1}	PRODUCTS
ARSENOPYRITE[1]	$1.7x10^{-6}$	0.9	18[a], -6[b]	SO_4^{2-}
GALENA[2]	$1.6x10^{-6}$	1.0	48	SO_4^{2-} (dom.), S_s
PYRITE[3]	$2.7x10^{-7}$	0.6	92	SO_4^{2-}
MARCASITE[3]	$1.5x10^{-7}$	-.-	-.-	SO_4^{2-}
BLAUBLEIBENDER COVELLITE[4]	$7.1x10^{-8}$	-.-	52	SO_4^{2-}, S_s
CHALCOPYRITE[1]	$9.6x10^{-9}$	0.4	63	SO_4^{2}
COVELLITE[4]	$9.4x10^{-9}$	-.-	58	SO_4^{2-}, S_s

[1] This study ([a] 0 to 25°C, [b] 25 to 60°C); [2] Chermak 1986; [3] Wiersma and Rimstidt 1984; [4] Walsh and Rimstidt 1986.
-.- Indicates the value was not determined.

mechanism is complex; containing several steps and perhaps branch reactions. The oxidation of all sulfide minerals probably involves a complex series of reactions (Rimstidt *et al.* 1986). Nordstrom (1982) argues that the oxidation of pyrite involves the transfer of several electrons and that usually only one or two electrons are transferred in a single step. Thus, for pyrite where seven electrons are transferred during the conversion of one atom of disulfide sulfur to sulfate, as many as seven elementary steps may be needed. The same argument applies to arsenopyrite since arsenopyrite oxidation also involves the transfer of seven electrons per anion. Second, this behavior suggests that the reaction path contains a branch where although one reaction path is dominant at all temperatures, the other becomes increasingly important at higher temperatures. For example, one or more arsenic species created in one branch of the reaction path may act to inhibit or catalyze the rate limiting step for the overall reaction (Figs. 10 and 11). For the inhibitor scenario, the activation energy of a side reaction producing an inhibitor, E_a(inh), is larger than the activation energy of the rate limiting step, E_a(rls). Figure 10 is a schematic diagram illustrating this process. In the catalyst scenario, the activation energy of a side reaction producing a catalyst, E_a(cat), is smaller than the activation energy of the rate limiting step. A schematic diagram illustrating this process is shown in Figure 11. Either of these scenarios could cause the rate of the overall reaction to decrease with increasing temperature resulting in the observed negative activation energy. Such unusual temperature dependence, with negative activation energies, has been reported in other complex reactions such as the chemisorption of gases on solids (Low 1960, see Fig. 30) and reactions in cool flames (Gray 1968 and Yang 1969).

In the mixed flow reactor experiments, the time for a reaction to reach a steady state varied depending on the sulfide mineral and the flow rate, ranging from 2.5 to 22 hours with flow rates from 4.9×10^{-5} to 7.3×10^{-6} kg sec^{-1} for chalcopyrite and from nine to 23 hours with flow rates from 6.7×10^{-6} to 8.3×10^{-6}

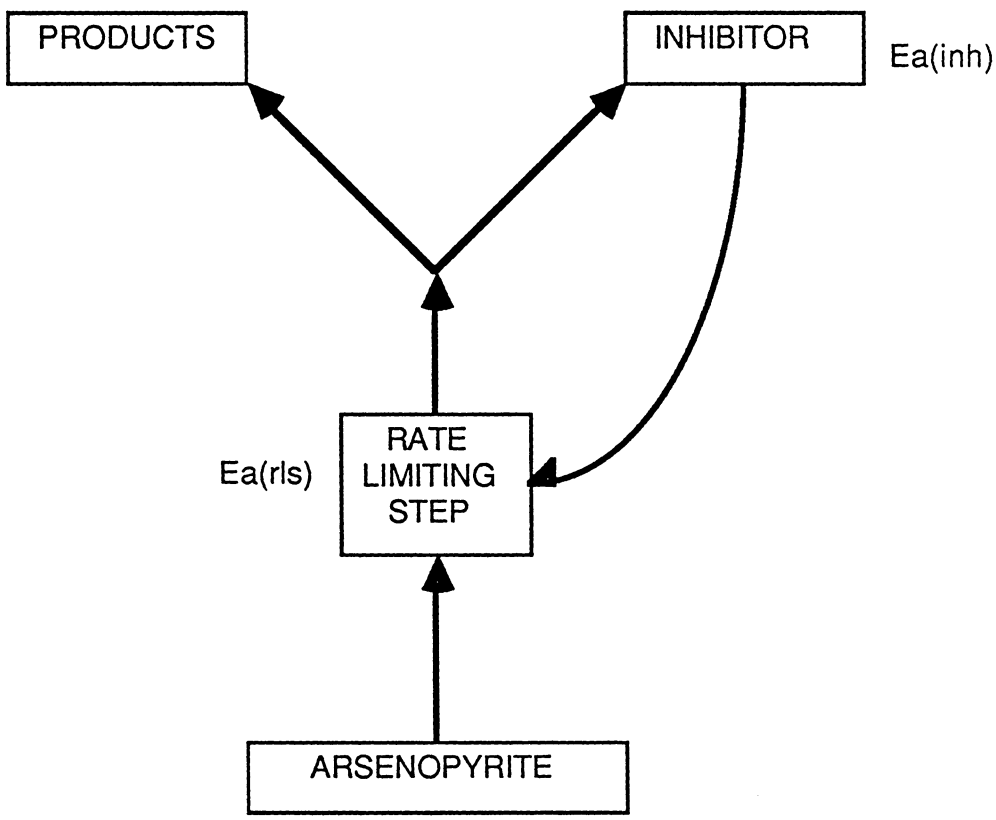

FIG. 10. Schematic diagram of proposed inhibitor mechanism for arsenopyrite oxidation.

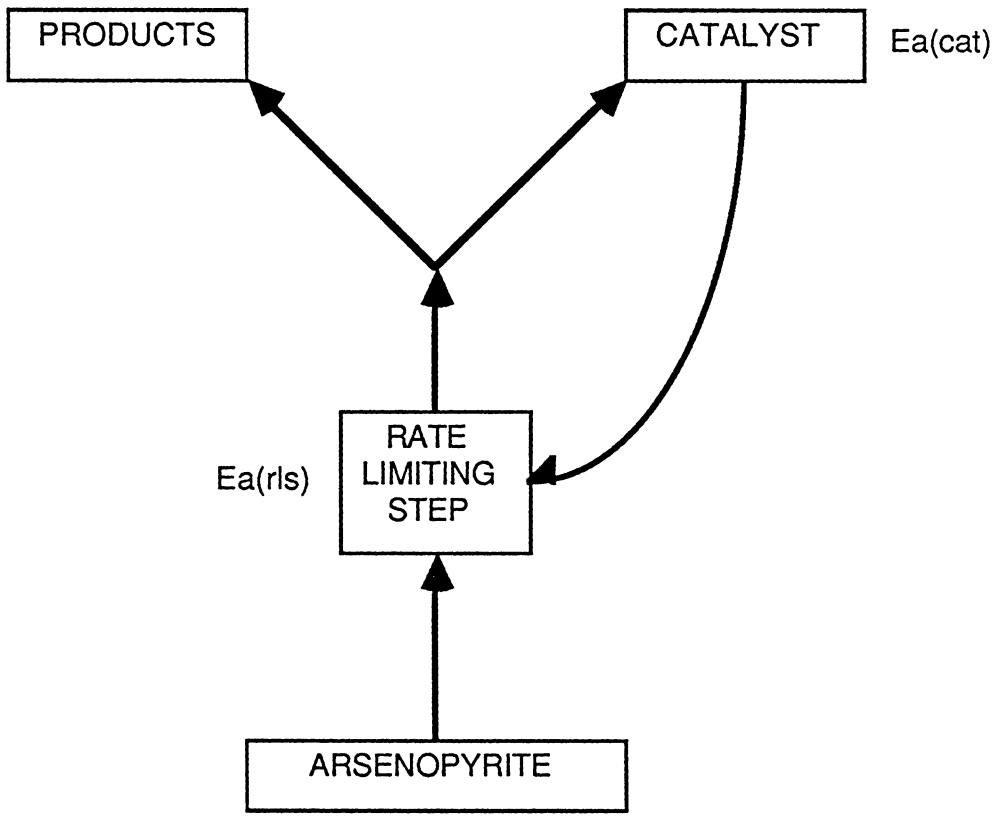

FIG. 11. Schematic diagram of proposed catalyst mechanism for arsenopyrite oxidation.

kg sec^{-1} for arsenopyrite. The chalcopyrite reaction produced Fe^{2+} concentrations very near the lowest detectable limit at 40°C. In order to increase the rate of production of Fe^{2+} more solids could be added or the flow rate slowed to get a greater extent of reaction (Chermak 1986). However, both of these have drawbacks. The slower flow rate does not allow enough fresh solution to dilute the reactor solution and thus this decreased fluid flow would increase the concentration of reaction products in the reactor, perhaps leading to their precipitation on the mineral surface where they would slow the reaction rate. The disadvantage of increasing the amount of solids is that all run solids may not be totally exposed to solution. The maximum flow rate is dictated by the minimum Fe^{2+} to Fe^{3+} ratio needed to give an accurate Eh reading. Best results were found when the experimental parameters of flow rate, surface area, initial ferric iron concentration, were adjusted so that the steady state emf value is in the range of 500 - 560 millivolts. Optimum results are obtained with ferric iron concentrations ranging from 10^{-2} to 10^{-5} molal (Chermak 1986). For iron concentrations of greater than 10^{-2} molal the amount of Fe^{3+} converted to Fe^{2+} is generally so small that a significant shift in Eh is not produced by the reaction. At ferric iron concentrations below 10^{-5} molal, the electrode does not respond solely to the ferrous/ferric couple (Natarajan and Iwasaki 1974). Sample size can probably range from 1 to 10 grams depending on the mineral's specific surface area and reaction rate (Chermak 1986).

In conclusion, the relatively slow rate of oxidation of chalcopyrite in acidic ferric iron solution indicates that further research is needed to increase oxidation rates and thereby, improve chalcopyrite hydrometallurgy. The relatively rapid rate of oxidation of arsenopyrite in acidic ferric iron solutions indicates that pollution problems from the drainage of sulfate and arsenic species from tailing piles containing significant amounts of pyrite and arsenopyrite could be serious.

REFERENCES

Beckstead, L. W. and Miller, J. D. (1977): Ammonia, oxidation leaching of chalcopyrite-reaction kinetics; *Metallurgical Transactions B*, **8B**, 19-29.

Berner, R. A. (1970): Low temperature geochemistry of iron, section 26 In *Handbook of Geochemistry*, II-1. Springer Verlag, Berlin.

Chermak, J. A. (1986): The rates of oxidation of galena and sphalerite in acidic ferric chloride solutions; M.S. Thesis, Virginia Polytechnic Institute and State University.

Dove, P. M. and Rimstidt J. D. (1985): The solubility and stability of scorodite, $FeAsO_4 \cdot 2H_2O$; *American Mineralogist* , **70**, 838-844.

Dutrizac, J. E. (1981): The dissolution of chalcopyrite in ferric sulfate and ferric chloride media; *Metallurgical Transactions B*, **12B**, 371-378.

Gray, B. F. (1968): Unified theory of explosions, cool flames and two-stage ignitions, part 1; *Ignitions and Cool Flames*, 1603-1613.

Habashi, F. (1978): Chapter 6, Aqueous oxidation I, *Chalcopyrite, Its Chemistry and Metallurgy*, McGraw Hill, 63-93

Habashi, F. and Tej Toor (1979): Aqueous oxidation of chalcopyrite in hydrochloric acid; *Metallurgical Transactions B*, **10B**, 49-56.

Haver, F. P. and Wong, M. M. (1971): Recovery of copper, iron, and sulfur from chalcopyrite concentrate using a ferric chloride leach; *Journal of Metals*, 25-29.

Langmuir, D. (1971): Eh - pH determination. In *Procedures in Sedimentary Petrology*, ed. R. E. Carver, John Wiley and Sons, New York, 597-635.

Leach, D. L. and Braun, R. L. (1975): Leaching of primary sulfide ores in sulfuric acid solutions at elevated temperatures and pressures; Lawrence Levermore Laboratory, University of California, UCRL- 75899.

Levenspiel, O. (1972): *Chemical Reaction Engineering*, 2nd edition. John Wiley and Sons, New York.

Low, M. J. D. (1960): Kinetics of chemisorption of gases on solids, *Chemical*

Reviews, **60**, 267-312.

McKibben, M. A. and Barnes, H. L. (1986): Oxidation of pyrite in low temperature acidic solutions: rate laws and surface textures, *Geochim. Cosmochim. Acta*, **50**, 1509-1520.

Munoz, P. B., Miller, J. D. and Wadsworth, M. E. (1979): Reaction mechanism for the acid ferric sulfate leaching of chalcopyrite; *Metallurgical Transactions B*, **10B**, 149-158.

Murray, R. J. (1972): *The dissolution of a galena concentrate in aqueous ferric-chloride solutions,* Ph.D. Thesis, Univ. of Idaho.

Natarajan, D. A. and Iwasaki, I. (1974): Eh measurements in hydrometallurgical systems. *Minerals Science Engineering*, **6**, 35-44.

Nordstrom, D. K. (1977): Thermochemical redox equilibria of Zobell's solution. *Geochim. Cosmochim. Acta*, **41**, 1835-1841.

Nordstrom, D. K. (1982): Aqueous pyrite oxidation and the consequent formation of secondary iron minerals. *Acid Sulfate Weathering*, **3**, 37-56.

Palmer, B. R., Nebo, C. O., Rau, M. F. and Fuerstenau, M. C. (1981): Rate phenomena involved in the dissolution of chalcopyrite in chloride-bearing lixiviants; *Metallurgical Transactions B*, **12B**, 595-601.

Pinches, A. (1975): Bacterial leaching of an arsenic-bearing sulfide concentrate, *Leaching and Reduction in Hydrometallurgy*; 28-35.

Rimstidt, J. D.; Chermak, J. A. and Newcomb, W. D. (1986): The oxidation of sulfide minerals; Fifth International Symposium on Water-Rock Interaction; Reykavik, Iceland, August 8-17, 471-474.

Rimstidt, J. D. and Dove, P. M. (1986): Mineral/solution reaction rates in a mixed flow reactor: wollastonite hydrolysis: *Geochim. Cosmochim. Acta.*, **50**, 2509-2516.

Walsh, C. A. and Rimstidt, J. D. (1986): Rates of reaction of covellite with ferric iron at pH 2. *Canadian Mineralogist*, **24**, 35-44.

Wan, R. Y., Miller, J. D., Foley, J. and Pons, S. (1985): Electrochemical features of

the ferric sulfate leaching of $CuFeS_2$/C aggregates; *Proceedings of the International Symposium on Electrochemistry in Mineral and Metal Processing*, **84**.

Wan, R. Y., Miller, J. D. and Simkovich, G. (1984): Enhanced ferric sulfate leaching of copper from $CuFeS_2$/C particulate aggregates; *International Conference on Recent Advances in Mineral Science and Technology*.

Wiersma, C. L. (1982): Relative rates of reaction of pyrite and marcasite with ferric iron at low pH. MS Thesis, Virginia Polytechnic Institute and State University.

Wiersma, C. L. and Rimstidt, J. D. (1984): Rates of reaction of pyrite and marcasite with ferric iron at pH 2. *Geochim. Cosmochim. Acta*, **48**, 85-92.

Yang, C. H. (1969): Two stage ignition and self-excited thermokinetic oscillation in hydrocarbon oxidation, *J. Phys. Chem.*, **73**, 3407-3413.

Yu, P. H., Hansen, C. K. and Wadsworth, M. E. (1973): A kinetic study of the leaching of chalcopyrite at elevated temperatures; *International Symposium on Hydrometallurgy*, Feb. 25- March 1, 375-402.

APPENDIX I

SURFACE AREA OF UNREACTED ARSENOPYRITE

The surface area of the unreacted arsenopyrite used in these experiments was determined using a two point N_2 BET isotherm obtained from a "Quantachrome" Quantasorb surface area analyzer. Three samples were analyzed twice and averaged for a mean surface area.

	sample 1	sample 2	sample 3
Surface Area:	0.062	0.066	0.073
	0.062	0.069	0.061

Mean: 0.066±0.002

APPENDIX II

REACTION RATES OF ARSENOPYRITE IN THE MFR

The arsenopyrite reaction rates measured using the mixed flow reactor, are given in Table 10 and plotted as log rate versus log $m_{Fe}3+$ in Figure 12. These data give a reaction order of 0.75±0.03. Figure 12 shows that the reaction rate decreases with increasing temperature in the 40 to 60°C range and in fact the calculated E_a is -20±6 kJ mol^{-1}. Further discussion of the significance of a negative activation energy may be found in the conclusions section of this paper.

TABLE 10. ARSENOPYRITE REACTION RATES (MFR)

RUN NUMBER	Fe^{3+} in molal	EMF volts	Fe^{3+} out molal	r_{pump} kg sec^{-1}	A_s* m^2 g^{-1}	MASS of SOLID, g	log r mol m^{-2} sec^{-1}
				40°C			
Aspy 41	1E-02	0.5252	1.3E-03	7.52E-06	0.17	2.0004	-6.709
Aspy 43	1E-03	0.5192	1.1E-04	7.25E-06	0.12	2.0013	-7.569
Aspy 44	1E-04	0.5011	5.6E-06	8.33E-06	0.10	2.0001	-8.425
Aspy 45	1E-04	0.5074	7.1E-06	7.58E-06	0.10	2.0001	-8.472
				60°C			
Aspy 49	1E-04	0.5122	8.4E-06	6.81E-06	0.12	2.0001	-8.599
Aspy 50	3.2E-04	0.5215	3.1E-05	6.67E-06	0.12	2.0007	-8.102

* Surface area of the reacted material (Appendix IV).

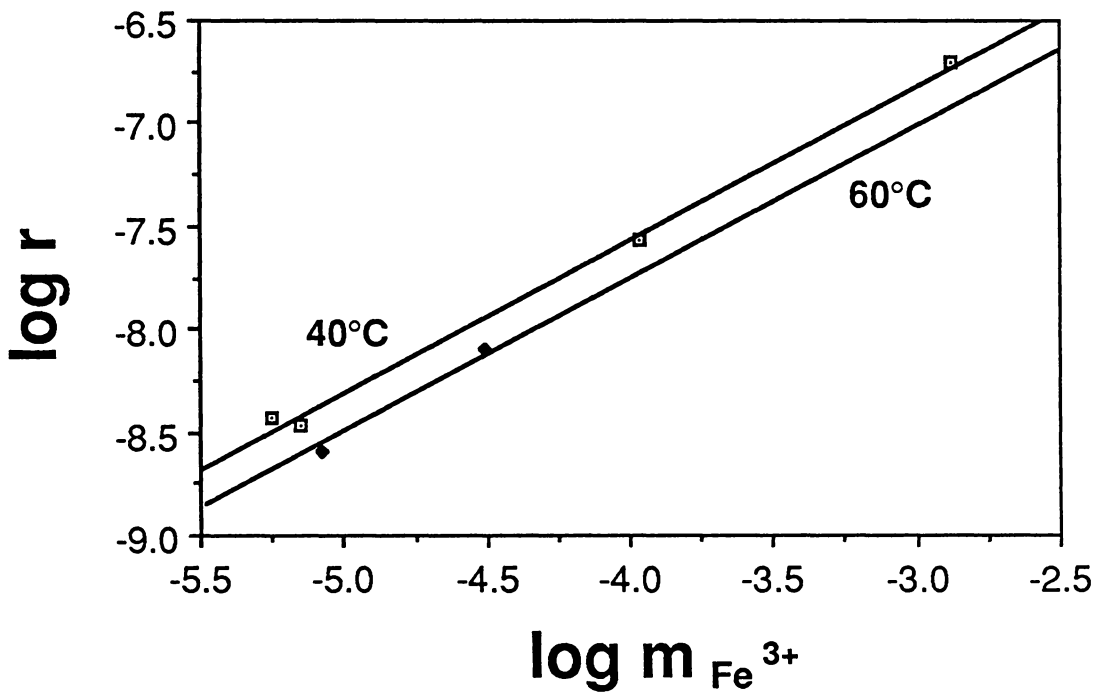

FIG. 12. Arsenopyrite oxidation rates plotted as log rate versus log $m_{Fe}3+$. The equation of best fit of all the data is:

$$\log r = -1028 \pm 290\ (1/T) + 0.75 \pm 0.03\ (\log m_{Fe}3+)$$

APPENDIX III
CHALCOPYRITE SURFACE AREA MEASUREMENTS

The surface area of the reacted chalcopyrite was determined by N_2 adsorption using a "Quantachrome" Quantasorb surface area analyzer. Due to time constraints only a few run samples were selected and analyzed. The precision for the measurements was found to be larger than the variance of the determined surface areas (see runs 17, 22 and 33). Consequently the average surface area of all measurements, 0.030±0.013, was used in calculating the rate of all the chalcopyrite runs. The individual measurements are listed below.

RUN #	SURFACE AREA
Cpy 16	0.027
Cpy 16	0.027
Cpy 17	0.045
Cpy 17	0.020
Cpy 17	0.040
Cpy 22	0.017
Cpy 22	0.052
Cpy 22	0.038
Cpy 23	0.032
Cpy 30	0.023
Cpy 32	0.022
Cpy 33	0.017
Cpy 33	0.015
Cpy 33	0.018
Cpy 34	0.058

APPENDIX IV

SURFACE AREA MEASUREMENTS FOR ARSENOPYRITE IN THE MFR

The surface area of the reacted arsenopyrite was determined using a two point N_2 BET isotherm obtained from a "Quantachrome" Quantasorb surface area analyzer. Each run sample was analyzed twice and the averages are given below.

RUN #	SURFACE AREA
Aspy 41	0.17
	0.17
Aspy 43	0.11
	0.13
Aspy 44	0.11
	0.10
Aspy 49	0.11
	0.13
Aspy 50	0.12
	0.12

APPENDIX V

INDUCTIVELY COUPLED PLASMA ANALYSIS OF EFFLUENT

Select samples of the final effluent of the mixed flow reactor experiments with chalcopyrite and arsenopyrite and solutions from batch reactor experiments with arsenopyrite were analyzed for iron, copper, arsenic and sulfur using inductively coupled plasma spectrometry. The results of these analyses along with molar ratios of Fe^{2+}/Cu or Fe^{2+}/As where applicable are listed in Table 11.

According to equation 1 the Fe^{2+}/As ratio should be 14/1, and according to equations 2 and 3 the Fe^{2+}/Cu ratio should lie between 17/1 or 5/1. The Fe^{2+}/As ratios are quite varied and only appear near 14/1 in one case. The Fe^{2+}/Cu ratios are quite varied, in some cases less than 5/1 and appear to decrease with decreasing concentration.

TABLE 11. INDUCTIVELY COUPLED PLASMA ANALYSIS OF EFFLUENT SOLUTIONS

RUN NUMBER	TOTAL IRON molal	COPPER molal	SULFUR molal	FERROUS IRON* molal	Fe^{2+}/Cu^{2+}
cpy 17	1.135×10^{-4}	5.926×10^{-6}	1.304×10^{-6}	6.967×10^{-5}	11.76
cpy 20	1.791×10^{-5}	3.964×10^{-6}	1.057×10^{-6}	1.704×10^{-5}	4.30
cpy 22	4.920×10^{-5}	4.258×10^{-6}	1.310×10^{-7}	3.951×10^{-5}	9.28
cpy 30	1.121×10^{-4}	6.496×10^{-6}	1.073×10^{-6}	7.425×10^{-5}	11.43
cpy 31	4.081×10^{-5}	6.293×10^{-6}	9.981×10^{-7}	3.447×10^{-5}	5.48
cpy 33	1.817×10^{-5}	5.039×10^{-6}	1.229×10^{-6}	1.766×10^{-5}	3.50
cpy 34	1.817×10^{-5}	5.050×10^{-6}	1.410×10^{-6}	1.768×10^{-5}	3.50

RUN NUMBER	TOTAL IRON molal	ARSENIC molal	SULFUR molal	FERROUS IRON* molal	Fe^{2+}/As
aspy 42	1.064×10^{-2}	1.015×10^{-3}	3.745×10^{-4}	9.318×10^{-3}	9.18
aspy 43	1.208×10^{-3}	1.326×10^{-4}	5.424×10^{-5}	1.100×10^{-3}	8.29
aspy 45	1.474×10^{-4}	4.634×10^{-5}	1.251×10^{-5}	1.403×10^{-4}	3.03
aspy 64	1.298×10^{-4}	2.966×10^{-5}	7.361×10^{-6}	1.102×10^{-4}	3.72
aspy 67	1.082×10^{-3}	7.750×10^{-5}	2.230×10^{-5}	8.300×10^{-4}	10.71
aspy 71	1.040×10^{-3}	1.943×10^{-5}	8.765×10^{-6}	3.741×10^{-4}	19.25
aspy 72	3.475×10^{-4}	1.397×10^{-5}	4.959×10^{-6}	1.912×10^{-4}	13.68
aspy 75	1.174×10^{-4}	1.193×10^{-5}	4.959×10^{-6}	7.555×10^{-5}	6.33

* Ferrous iron concentrations were calculated from the total iron concentrations and the solution Eh at the time of sampling using equation (9).

The vita has been removed from the scanned document